



Petrographic and Geochemical Studies of the Host Rock of the Chagho Copper Orebody in the Southwest of Karaj

Estudios Petrográficos y Geoquímicos de la Roca huésped del Yacimiento de Cobre Chagho en el Suroeste de Karaj

Alireza Rakhshani Moghadam¹, Mohammad Lotfi¹, Mohammad Reza Jafari¹, Afshin Ashja-Ardalan¹, Majid Pour Moghaddam², Abdollah Yazdi^{*3}

¹Department of Geology, North Tehran Branch, Islamic Azad University, Tehran, Iran.

²Department of Education, Ministry of Industry Mines and Trade, Tehran, Iran.

³Department of Geology, Kahnooj Branch, Islamic Azad University, Kahnooj, Iran.

* yazdi_mt@yahoo.com

(*recibido/received: 20-mayo-2021; aceptado/accepted: 13-agosto-2021*)

ABSTRACT

The study area is located 5 km southwest of Mahdasht city in Karaj on the Urmia-Dokhtar magmatic arc. In this area, Eocene volcanic and pyroclastic rocks are observed including basaltic andesite lavas, andesite, Trachyandesitic and trachyte lavas, tuff, and ignimbrite, along with plutonic rocks. There are two spectra of basic and acidic for the rocks in the area, of which basic rocks are chemically calc-alkaline in nature. Among the signs of subduction rocks in the area are enrichment in the Ta, Nb, and Ti lavas, as well as the anomaly of the HFSE index relative to the LILE of incompatible elements content. The geochemical and petrogenetic studies indicate the origin of the area's plutonic rocks and the role of differential crystallization accompanied by the crustal rocks-contamination and digestion of magma in the evolution of the magma forming these rocks. This magma has been originated from the low-grade partial melting of an enriched mantle origin beneath the continental lithosphere with the Iherzolite garnet composition at a depth of 100 to 110 km in a post-collision tensile environment. Investigating the fluids involved in the region, the homogenization temperature with the temperature of copper veins formation is between 120 to 306 ° C, with the salinity percentage varying between 6.45 to 15.96% of sodium chloride weight. Accordingly, this metamorphic hydrothermal orebody is located in the mesothermal category. The presence of sub-faults, joints, and cracks in the host rock has provided a low-pressure environment for a proper place for copper mineralization as veins.

Keywords: Petrology, Geochemistry, Urmia-Dokhtar zone, Copper orebody, Chagho, Iran.

RESUMEN

El área de estudio se encuentra a 5 km al suroeste de la ciudad de Mahdasht en Karaj en el arco magmático Urmia-Dokhtar. En esta zona se observan rocas volcánicas y piroclásticas del Eoceno que incluyen lavas de andesita basáltica, lavas de andesita, traquiandesita y traquita, toba e ignimbrita, junto con rocas plutónicas. Existen dos espectros básicos y ácidos para las rocas de la zona, de las cuales las rocas básicas son químicamente calco-alcalinas por naturaleza, entre los signos de subducción en la zona se encuentran el enriquecimiento en las lavas de Ta, Nb y Ti, así como la anomalía del índice HFSE relativo al LILE de contenido de elementos incompatibles. Los estudios geoquímicos y petrogenéticos indican el origen de las rocas plutónicas de la zona y el papel de la cristalización diferencial acompañada de la contaminación y digestión de las rocas de la corteza en la evolución del magma que forma estas rocas. Este magma se ha originado a partir de la fusión parcial de bajo grado de un origen de manto enriquecido debajo de la litosfera continental con la composición de granate lherzolita a una profundidad de 100 a 110 km en un entorno de tracción posterior a la colisión. Investigando los fluidos involucrados en la región, la temperatura de homogeneización con la temperatura de formación de vetas de cobre está entre 120 a 306 ° C, con un porcentaje de salinidad que varía entre 6.45 a 15.96% del peso de cloruro de sodio. En consecuencia, este cuerpo mineral hidrotermal metamórfico se encuentra en la categoría mesotérmica. La presencia de sub-fallas, juntas y grietas en la roca huésped ha proporcionado un ambiente de baja presión para un lugar adecuado para la mineralización de cobre como vetas.

Palabras clave: Petrología, Geoquímica, Zona Urmia-Dokhtar, Yacimiento de cobre, Chaghoo, Irán.

1. INTRODUCCIÓN

The studied rocks include a wide series of lavas and Middle and Upper Eocene pyroclastic and sedimentary rocks outcropped with an almost east-west trend. The Middle Eocene combination mostly consists of green pyroclastic rocks composing of tuff sandstone, green tuff, limestone tuff, and red tuff conglomerate. The Upper Eocene complex consists of two acidic and basic phases operating alternately in three stages. The basic phase is composed of rocks with moderate to basic chemical composition such as andesites, Trachyandesitic (sometimes quartzitic), pyroxene-containing andesites, basalt, and Trachy-basalt along with related tuffs (Figure 1 and 2). The acidic phase contains rhyolite and rhyodacitic and quartz-trachytic ignimbrites, cuts, and tuffs with the same composition as well as rhyodacitic lavas (Pourabdollahi et al. 2021). After the Eocene and possibly at the start of the Oligocene, granitic-quartz-monzonite plutonic masses penetrated the lower Eocene rocks to a limited extent, which were cut by diabasic (doleritic) dikes. There are three completely separate zones in the study area in terms of structural geology (Olufemi et al. 2020; Ullah et al. 2021; Saeedi Razavi 2021; Barahouei et al. 2021; Arampour et al. 2021). The northeastern part of the map is located in the central Alborz zone with the southern and central part located in the central Iran zone. The border between Alborz and central Iran is the Eshtehard subsidence, which is originated from the thrust of northern Tehran in the east-west direction to the northwest-southeast considered as the continuation of the Tehran plain. Furthermore, the traces of Urmia-Dokhtar zone units are also observed in the area (Adewumi et al. 2021; Gardezi et al. 2021; Rajabi et al. 2021; Jafari et al. 2021; Morovati et al. 2021). The most important alterations in the Chaghoo copper range include siliceous, moderate argillic and

sericitic alterations, and propylitic in some points. However, siliceous alteration is predominant in the study area and it is almost the most important sign of copper orebodies.

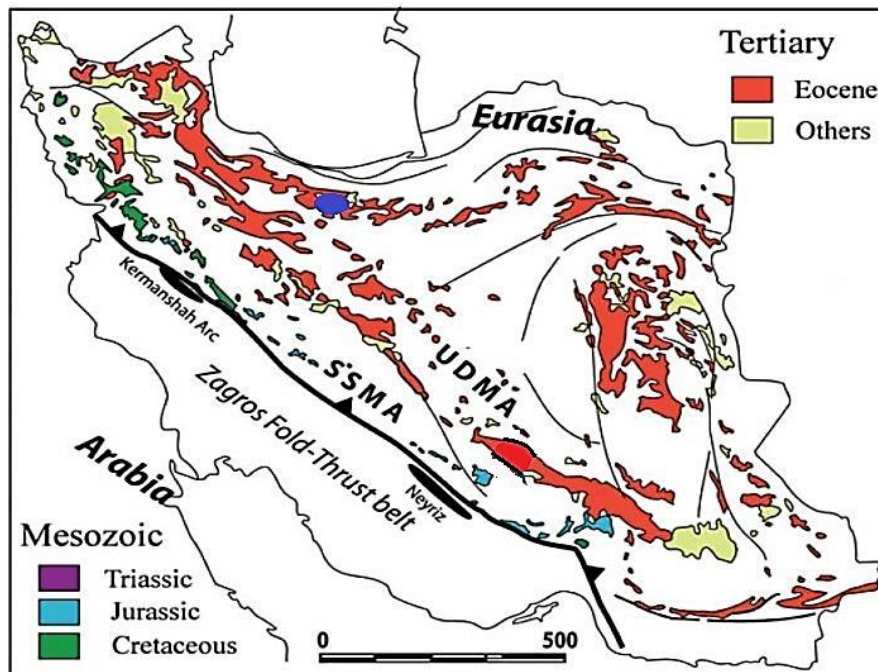


Figure 1. The studyarea in the map of structural zones of Iran (Agard et al., 2011).

2. METHODOLOGY

The studies in this research were performed in the field and laboratory parts. In the field part, the lithological characteristics of the host rock, mineralization events, and discontinuity relationships between the phenomena were evaluated and the host rock and mineralization sections were sampled based on histological changes and lithology. The laboratory studies were carried out aimed at lithographic investigations and determination of alteration and mineralization complexes. To assess and identify secondary or minor elements 9 samples were selected through the Inductively Coupled Plasma Mass Spectrometry (ICP-MS) method, from the Northern Chghoo area rock index samples and 6 samples were chosen from the Southern Chaghoo area. The tests (ICP-MS) have been performed by Zarazma Mineral Studies Company.

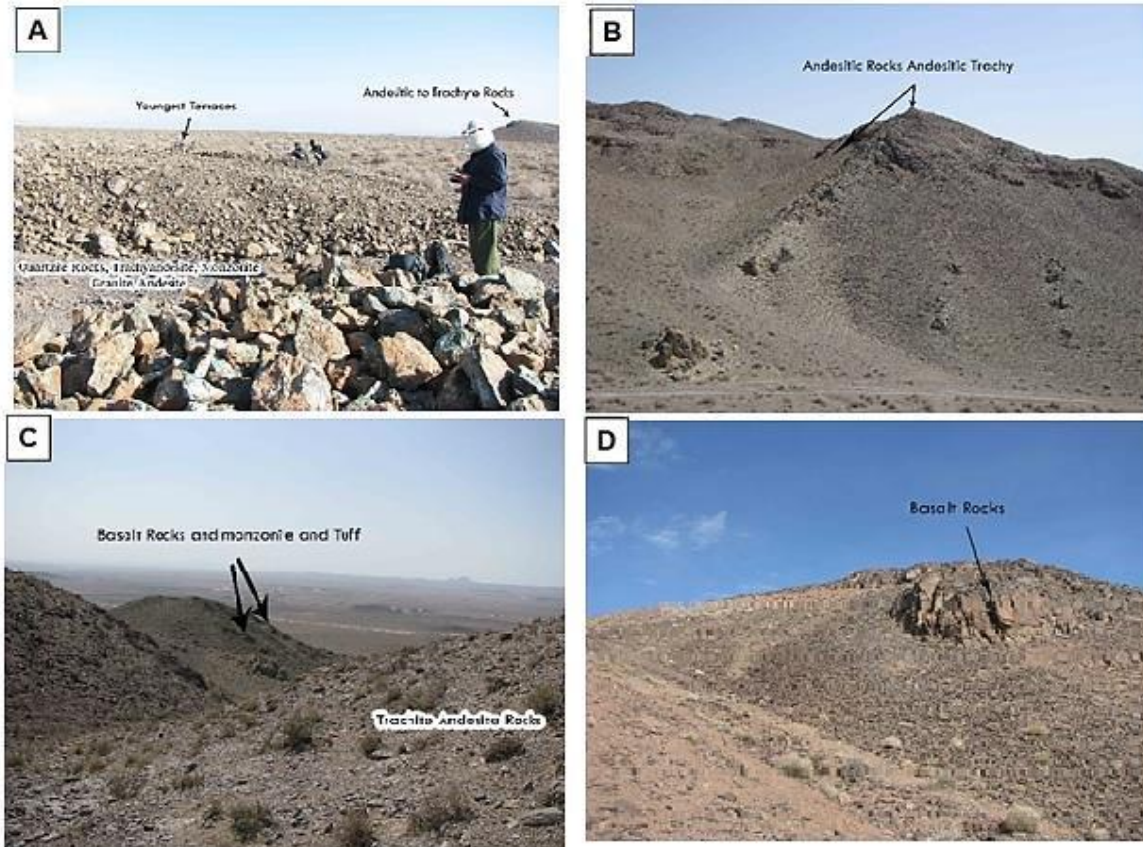


Figure 2. A) The andesitic rocks and surrounding alluvial terraces, B) and C) The basaltic and andesitic rocks in the northern Chaghoo, D).The basaltic rocks in the southern Chaghoo.

3. GEOLOGY OF THE STUDY AREA

The orebody is located near the Chaghoo village and contains two mineral origins, one in the northeast and the other in the south. The magmatic rocks in this area include plutonic rocks (e.g., granite, quartz syenite, quartz monzonite) and volcanic rocks (such as rhyolite, quartz, Trachyandesite, andesite, Trachyandesitic alkaline basalts, Trachyandesiticbasalt, basalt, and olivine basalts). The rock units of the area include andesite, trachyandesitic, trachybasalt with the Eocene age.

Andesite: These rocks are dark gray and dark turquoise in the samples. Regarding petrographic features, this rock unit contains plagioclase and pyroxene crystals in porous and glomeroporphyritic glassy texture. Plagioclase phenocrysts make the largest volume of these rocks, where the rotation of ferrous solutions is occasionally observed in their fractures.

Trachyandesite: In the northern Chaghoo area and the hand samples, it is found in gray to light brown. It has a porphyric texture, in which the plagioclase phenocrysts are observed with a mixture of andesine with albite-Carlsbad twins along with zoning. Chlorite and epidote minerals

are also found in these rocks (Figure 3-B). Opaque and apatite minerals are among the secondary minerals of these rocks.

Basaltic rocks: They include olivine basalt, basalt, and alkaline basalts. The predominant textures in these rocks are porphyritic, glomeroporphyritic, amygdaloidal, and microlithic. These rocks mainly comprise plagioclase, clinopyroxene, and olivine, and opaque minerals can also be seen in the matrix in addition to these minerals. The plagioclase crystals in tiny to medium sizes, are often automorphic and sub-automorphic, elongated, and rectangular, and have a macula polysynthetic, Carlsbad, and sometimes a degraded margin and even albite. Fine-grained olivine crystals are normally sub-automorphic and have been altered to biotite, serpentine, chlorite, iron oxide, and iddingsite. The matrix is composed of glass, plagioclase microlites, and opaque minerals along with sub minerals (Figure 3-D).

The studied plutonic rocks also include granite, quartz syenite, and quartz monzonite. These rocks with a granular texture (granular), mineralogically contain plagioclase, quartz, orthosis, pyroxene, chlorite, iron-carbonate hydroxides, and opaque minerals (Figure 3-A).

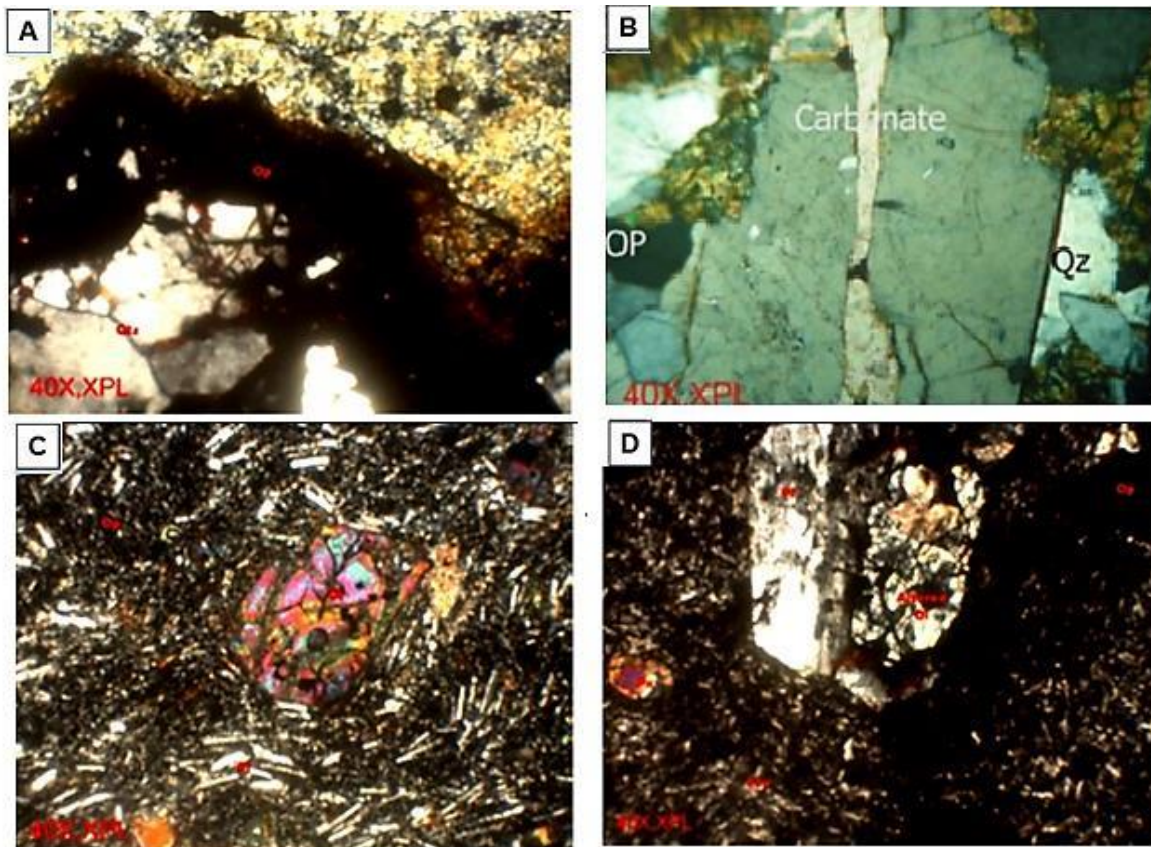


Figure 3. A) The granular texture in quartz monzonite., B) The presence of quartz and opaque minerals in rhyolite, C) The presence of opaque, pyroxene-altered olivine and plagioclase in trachandesitic basaltic, D) Altered olivine in olivine basalt.

4. MINERALOGRAPHIC FEATURES OF CHAGHOO AREA ROCKS

In trachyandesite rocks, metallic minerals are found including magnetite (3%), titanium oxide, and iron hydroxide. No traces of primary minerals is observed, therefore, the type of the primary mineral cannot be determined. These grains were probably pyrite or magnetite, substituted by limonite and goethite due to supergene alteration (Figure 4-A). In andesitic rocks, the abundance of magnetite is about 5%. The magnetite crystals are disseminated in the sample. Their size range is in 2-100 μm , however, most grains are less than 50 μm in size (Figure 4-B). Magnetites are found in both the matrix and the phenocrysts, however, in rhyolites, metal minerals include magnetite and iron hydroxide. Magnetites are intact with no signs of alteration or weathering (Figure 4-C). Iron hydroxides (i.e., limonite and goethite) have been replaced by a primary automorphic mineral. No trace of the original mineral was found and only the frame remained. These grains were probably pyrite substituted by iron hydroxides through supergene alteration. In basalts, metal minerals include magnetite (5%) and hematite. The automorphic crystals of this mineral with dimensions of 2 to 200 μm are disseminated in the sample. Some of the magnetites are replaced by hematite due to alteration (Figure 4-D).

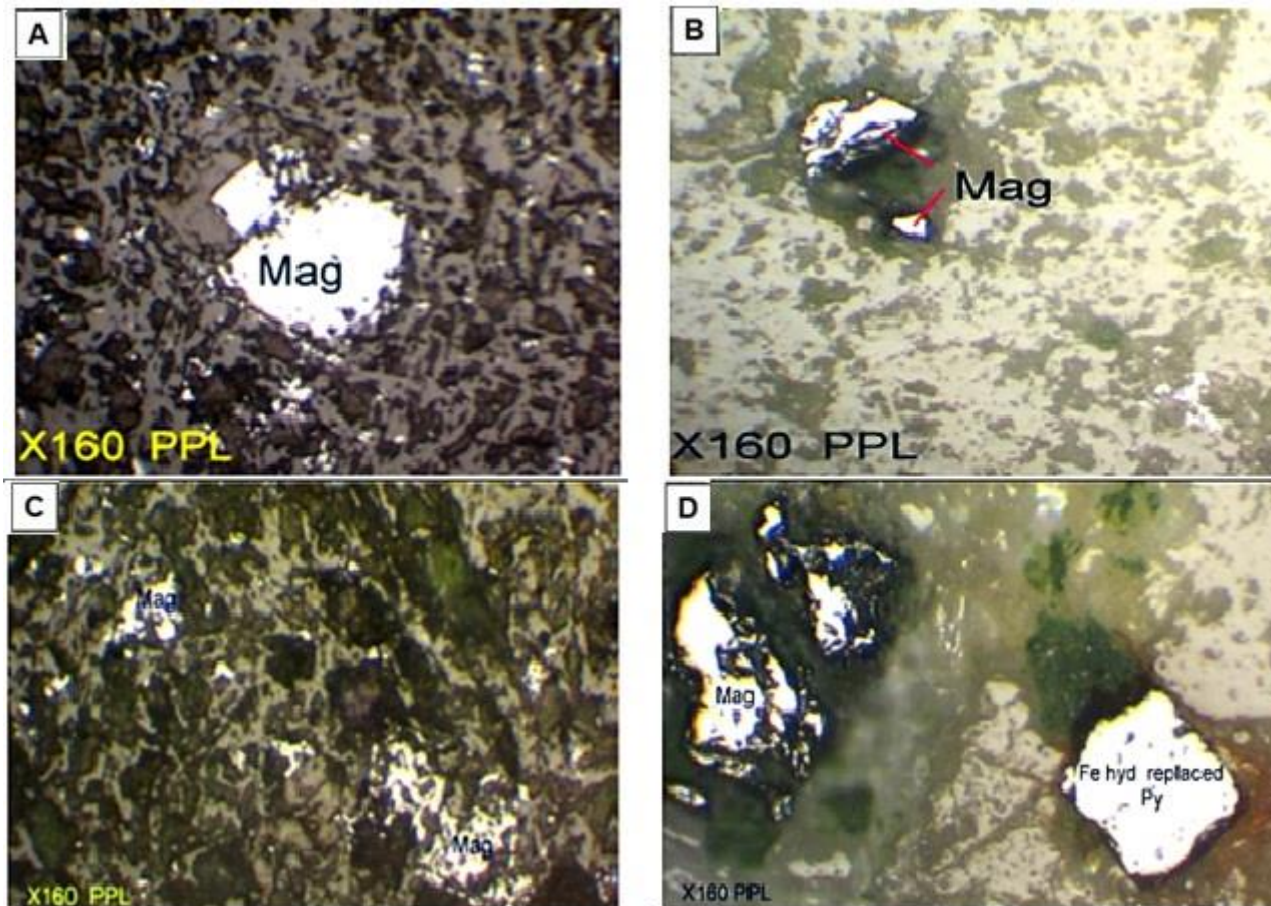


Figure 4. The metal minerals in rocks of the area: A) Trachyandesite, B) Andesite, C) Rhyolite, D) Basalt.

5. GEOCHEMICAL ASSESSMENTS OF THE ROCKS IN THE STUDY AREA

Studying the main elements of the rocks reveals that the rocks are within basic to moderate volcanic rocks. SiO₂ content in these rocks is 45 to 70%, which can be divided into 4 groups of basaltic rocks, trachyandesitic andesitic basalts, trachyandesitic, and rhyolite based on the TAS diagram (Figure 5-A and 5-B). Furthermore, based on the semi-alkaline and alkaline series categorization (Irvine & Baragar, 1971), the studied rocks are placed in the alkaline class (Figure-5). The content of major elements, such as Al₂O₃ and SiO₂, increases by decreasing MgO during magmatic differentiation. However, the major elements such as CaO and Fe₂O₃ decrease by reducing MgO levels. Zr has very low mobility during alteration (Le Roex et al., 1983; Talusani, 2010; Widdowson et al., 2000; Widdowson, 1991), moreover, this element has a wide range of variations in basaltic rocks. Furthermore, this element has a completely incompatible geochemical behavior during partial melting and differential crystallization in basaltic melts (Talusani, 2010) as well as a strong tendency to enter and remain in the melted phase.

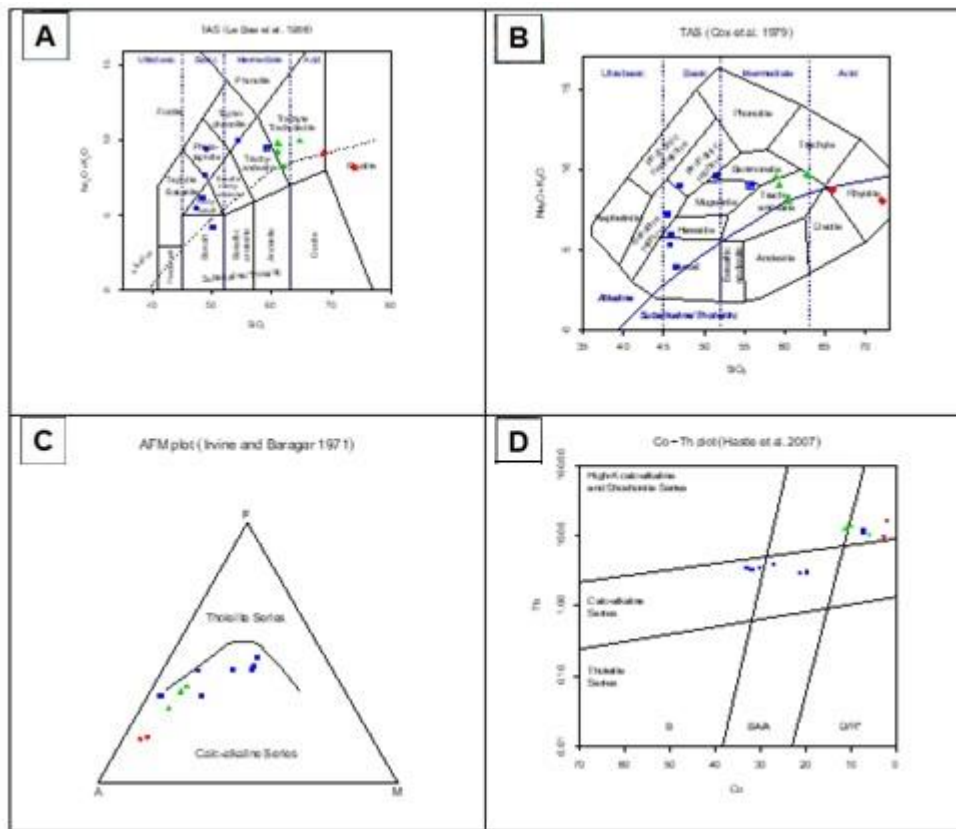


Figure 5. A) The diagram of Na₂O + K₂O versus SiO₂ (Cox et al., 1979). B) The diagram of Le Bas et al., (1986), C) The diagram of Hestie et al., (2007), D) The AFM diagram of Irvine and Baragar (1971).

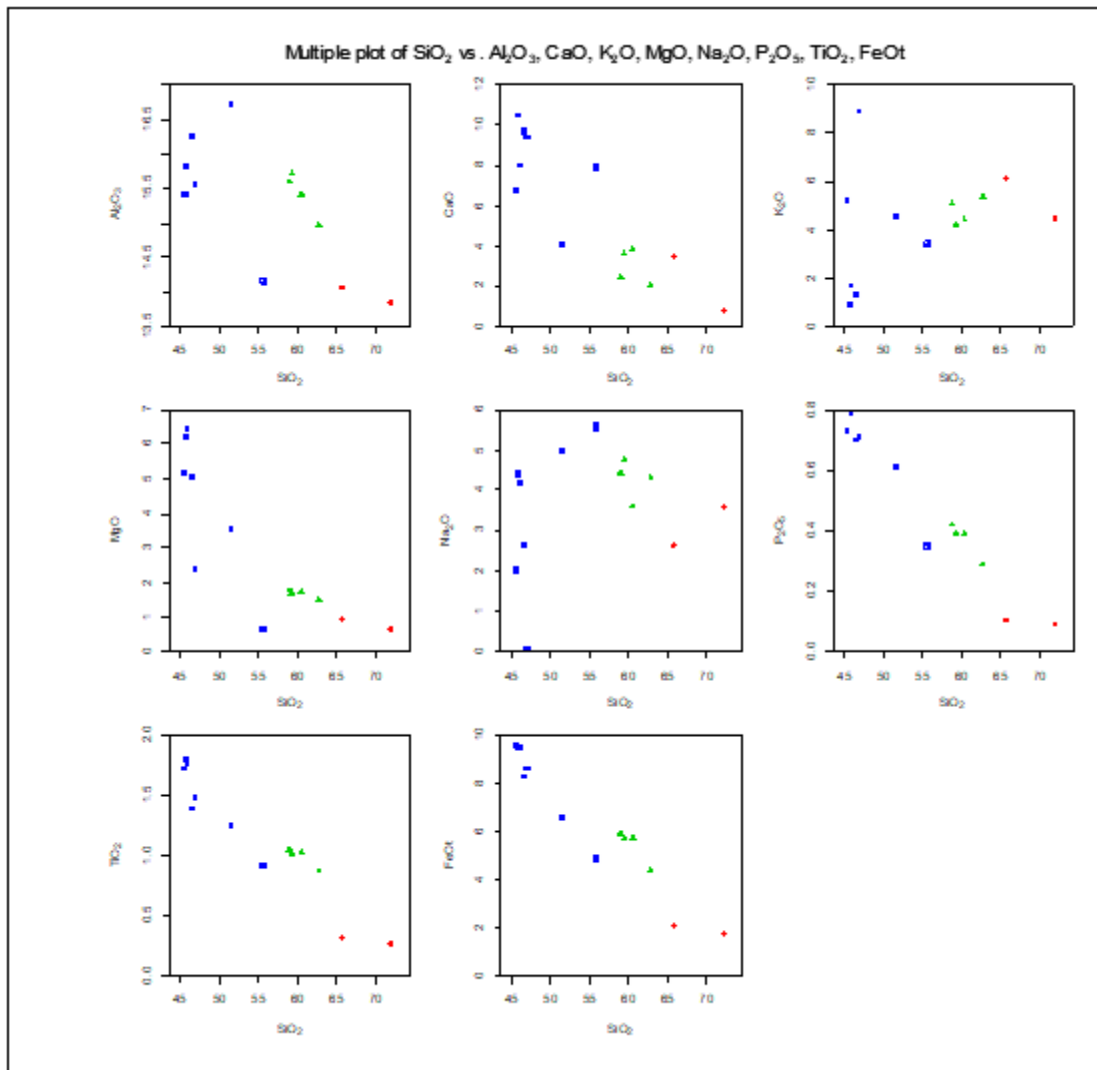


Figure 6. The Harker diagram of rocks in the study area.

The diagrams in Figure 7 represent the pattern of the mean normalized rare elements and rare earth elements (REEs) relative to the initial mantle and OIB values for the rocks in the study area. In all these diagrams, similar distribution patterns of elements in the rocks of the region are observed well. Some positive and negative anomalies are seen in the values of Sr, Rb, Nb, Pb, and Ba in the normalized diagram relative to the values of the primary mantle (Figure 7-A and 7-B). Since Ti and P are among the elements with high field stability strength (HFS) and do not show mobility during secondary processes, the observed anomalies can be interpreted based on petrological reasons. The negative anomaly in Nb also denotes the role of magmatic contamination with the continental crust in the evolution of the studied rocks. The severe positive anomaly of Pb and Ba represents continental crustal contamination and the positive Sr anomaly indicates the presence of plagioclase phenocrysts in the rock. The positive anomaly is associated with the Th, the increase of which indicated the crustal contamination. Therefore, to compare the composition of these rocks with arc and the back-arc samples of the Japanese magmatic against

the depleted diagonal composition was studied. The similarities and differences between the graphs represent the lack of maturity in the back-arc zone of the study area. Based on the diagram (Pearce, 1982), the samples are placed in a volcanic arc position (Figure 7). The studied samples are located in the magmatic arc zone (Figure 8-B and 8-C) in the diagrams (Wood et al., 1980).

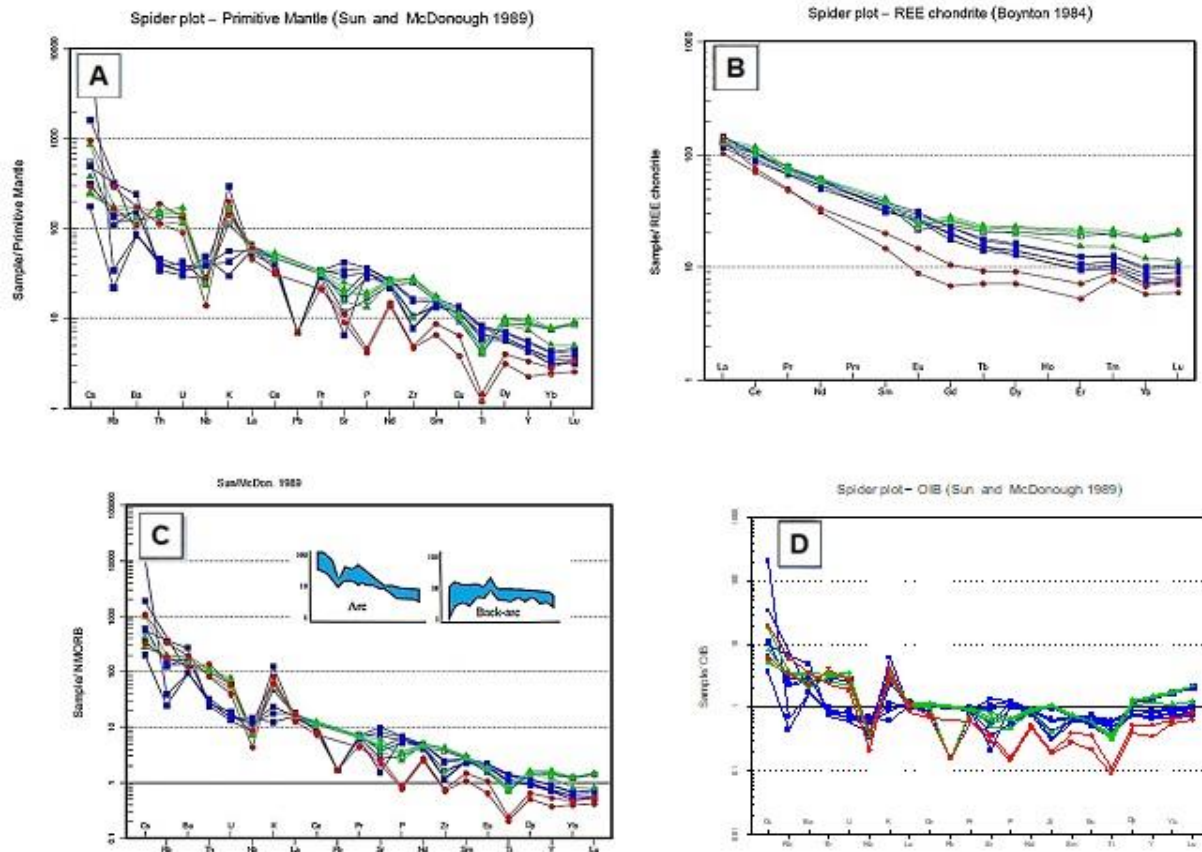


Figure 7. A) The normalized diagram of the samples relative to Chondrite (Nakamura, 1974), B) The normalized diagrams of samples relative to the primary mantle (Sun and McDonough, 1989), C) The normalized diagram relative to OIB, D) The diagram normalized to NMORB and its comparison with the pattern of the magmatic arc and back-arc of the supplementary Japanese arc of Poulet et al., (1994).

In the diagram of Aldanmaz et al. (2000) for the changes in the La/ Sm ratio to La, the continuous and dashed lines represent the trend of altering the composition of molts originated from different levels of partial melting of the spinel mantle of Lherzolite and Garnet-Lherzolite (Figure 8). The numbers on the lines represent the degree of partial melting. The range of the primary depleted and enriched mantle is clear on the thick line. Based on this figure, assuming a Lherzolite composition for the mantle, the trend of changes in the composition of molts can be traced that are derived from various degrees of mantle partial melting in two different series of depleted and enriched mantles. Regarding the abundance of La and Sm elements, all the studied basalt samples have a composition similar to the enriched mantle-derived melts and are placed on a process consistent with the partial melting of about 5% of garnet-containing lherzolite. The origin of

spinel-containing lherzolite is also confirmed in the LaN/ SmN versus TbN / YbN diagram (Wang et al., 2001). Regarding the location of the studied rocks in this diagram, the mantle has often spinel-lherzolite composition originating from a depth of 60 to 70 km corresponding to a pressure of 18 to 20 kb, which is the stability range of spinel.

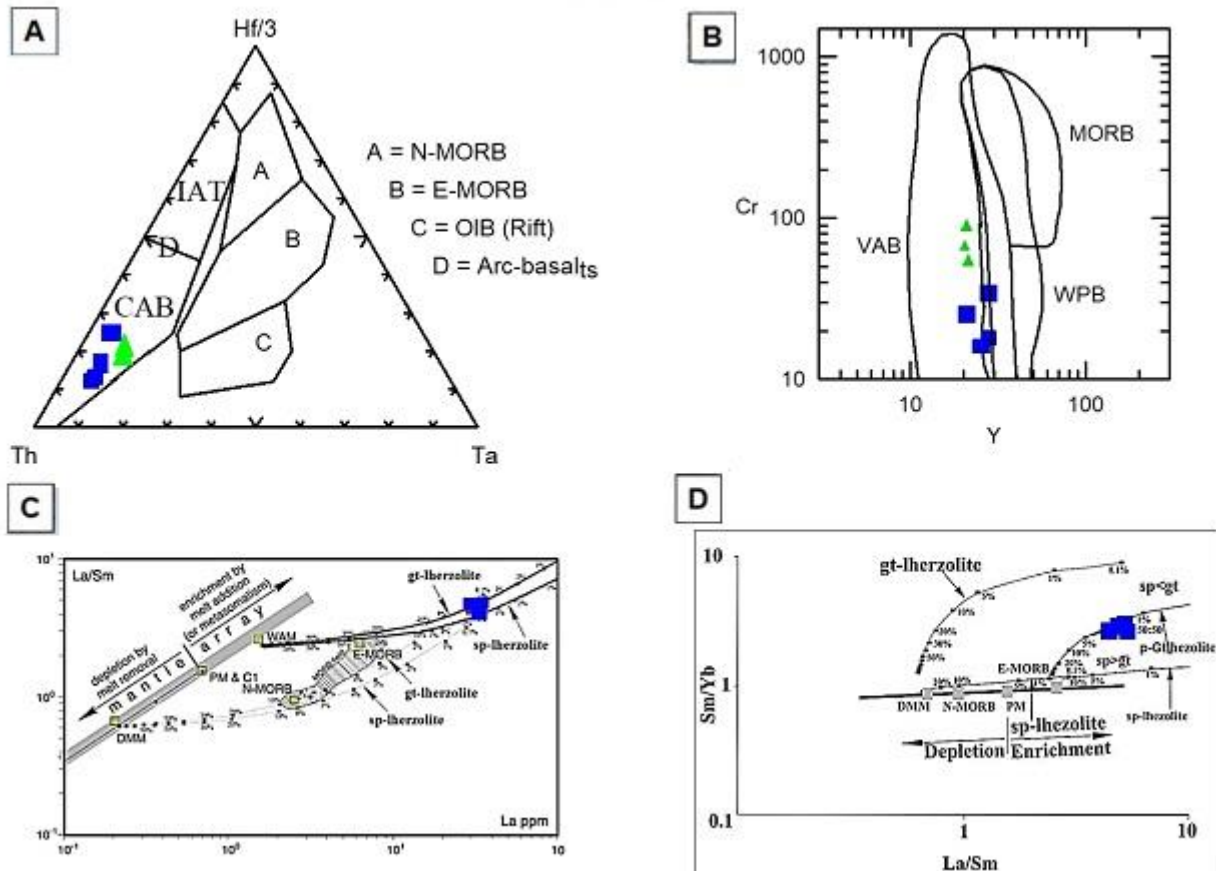


Figure 8. A) The position of the studied samples in the Cr versus Y diagram (Pearce, 1982), B) The triple diagrams for determining the tectonic environment (Wood et al., 1980), C) The Sm/ Yb against La/ Sm diagram for which the melting curves are based on the lherzolitic spinel mantle and the lherzolitic garnet mantle, and the samples are located within the garnet-containing lherzolite spinel (Shaw, 1970), D) The diagram of variations in the ratio of La/ Sm to La (Aldanmaz et al., 2000).

1-The mineralization systems of veins around porphyric orebodies are generally divided into epithermal and mesothermal groups (Corbett, 2004; Guilbert and Park, 1986). The type of such systems mineralization can be determined based on alteration, mineralogy, geochemistry, fluid, and isotopic shortcut data. Mineral paragenesis in the northeastern part of the Chaghoo orebody includes pyrite, chalcopyrite, bornite, malachite, azurite as well as chalcopyrite, malachite, and azurite in the southern part. The vein-type mineralization in this region has been originated from mineral-bearing fluids resulting from the post-magmatic activity of a subvolcanic mass. The

plutonic mass in this orebody is porphyritic quartz penetrating Eocene volcanic rocks and causing mineralization.

2-Based on the lithostratigraphic position, the replacement and infiltration of the subvolcanic mass may be related to the Pyrenees orogenic phase occurring between the Late Eocene and the Early Oligocene. The homogeneous temperature range of the copper veins is different between 123 to 319 ° C, moreover, the fluid salinity is between 15.7 to 17.2% of weight equivalent to the sodium chloride percentage. The depth of the mineral-bearing fluid is between 40 and 1100 m relative to the static surface and the pressure on the fluid is between 10.6 and 291 b. Accordingly, the orebody is placed in the mesothermal category. In general, the mineralization is of mesothermal type in this region associated with oxide and supergene mineral production in higher horizons owing to shallow features.

6. PRESENTING A GEODYNAMIC MODEL FOR THE FORMATION OF IGNEOUS ROCKS IN THE STUDY AREA

Slab melting has been proposed as a mechanism for generating Tertiary volcanism in Iran (Aftabi and Atapour, 2000; Omrani et al., 2008). Geochemical data taken as a whole do not support Paleogene slab melting, nor does slab melting explain the inland position of the Tertiary arc or synvolcanic extension and subsidence. Subsequent Tertiary volcanism was distributed over a large area (encompassing the Urumieh-Dokhtar belt, the Alborz Mountains, large parts of eastern Iran, and many relatively small locations in central Iran) but generally occurred between Cretaceous igneous rocks to the north and Triassic-Jurassic plutons to the south. The record of arc volcanism in Iran encompasses not only the well-defined belt of Paleogene calc-alkaline volcanics in the Urumieh-Dokhtar arc, but is widespread across Iran and spans roughly 175 Myr (Verdel et al., 2011).

This mechanism accounts for many of the characteristics of the Eocene flare-up: the inland position of the Urumieh-Dokhtar belt relative to the Late Triassic-Jurassic arc, synextensional volcanism, development of shallow submarine basins, and the asthenosphere-like geochemical affinity of the Oligocene basalts. However, Eocene volcanism, which was much more voluminous than Oligocene volcanism, had trace element compositions that are typical of arcs, not back arcs, and accumulated in the same basins as the Oligocene basalts. These first-order observations of the magmatic flare-up can be most simply explained as resulting from a hybrid of two common end-member mechanisms for generating volcanism: hydration of the mantle wedge by slab fluids as in subduction zones and decompression melting as in midocean ridges (Plank and Langmuir, 1988; Pearce and Parkinson, 1993; Sisson and Bronto, 1998; Conder et al., 2002; Gaetani and Grove, 2004). We propose the following four-stage model for the Eocene magmatic flare-up and subsequent Oligocene magmatism, which is broadly similar to the model of Humphreys et al. (2003) (Figure 8-A).

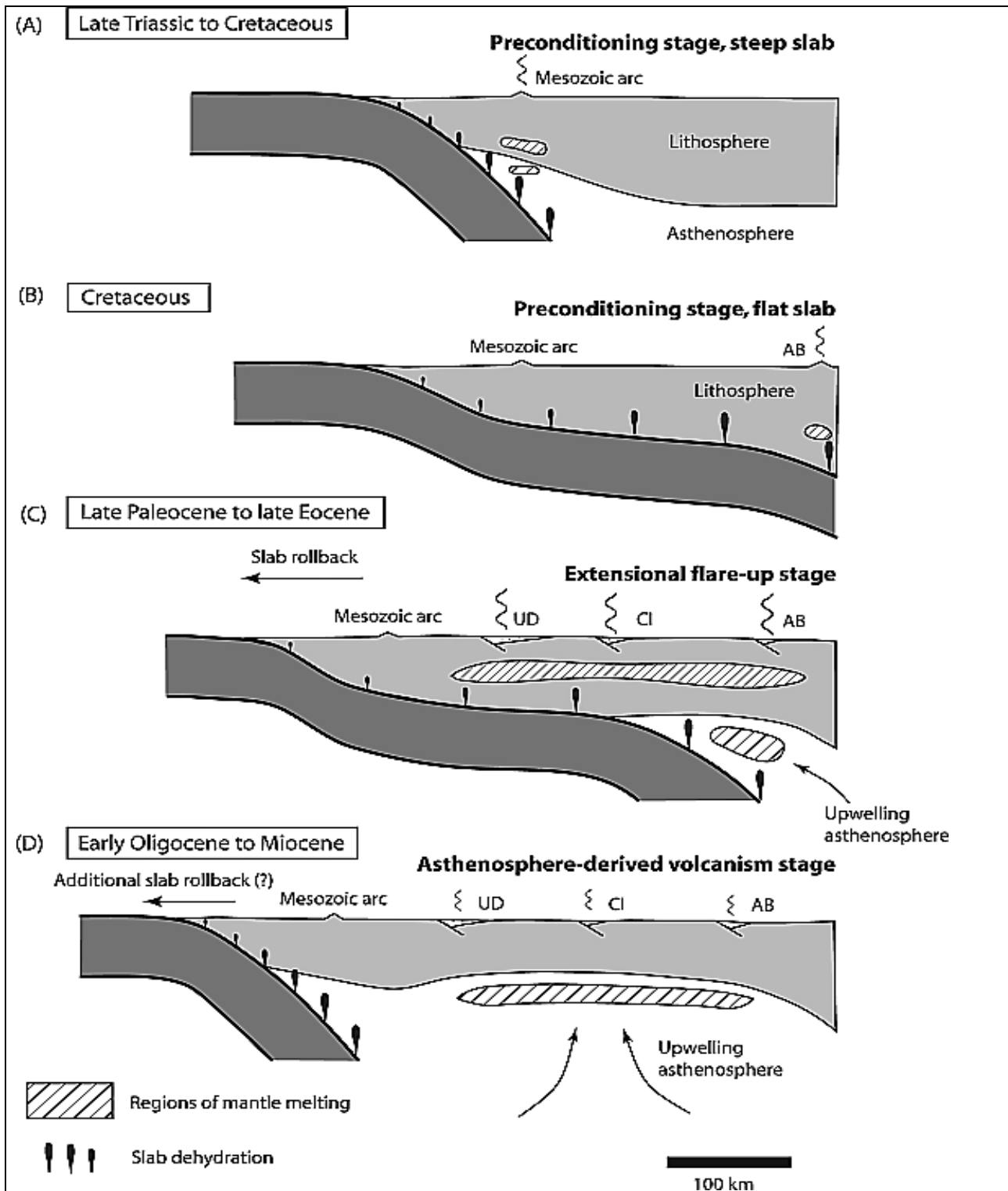


Figure 9. Summary of the development of the Iranian Eocene flare-up and subsequent asthenosphere-derived Oligocene magmatism.

Summary of the development of the Iranian Eocene flare-up and subsequent asthenosphere-derived Oligocene magmatism (Figure 9). (a) Late Triassic to Cretaceous slow subduction

generated limited magmatism within the Sanandaj-Sirjan zone. (b) Cretaceous flat slab subduction shifted the locus of magmatism to the Alborz Mountains. During this and the earlier stage, lithospheric mantle beneath the overriding plate was preconditioned by dehydration of subducted Neotethyan oceanic crust. (c) Late Paleocene to late Eocene slab rollback extended and thinned the overriding plate, leading to decompression melting of preconditioned lithospheric mantle and the formation of metamorphic core complexes and elongate rift basins. Magmatic contributions from upwelling asthenosphere were overwhelmed during this stage by the contribution from the fertilized lithospheric mantle. (d) Extension continued during the late Oligocene to Miocene during deposition of the Qom Formation. The flare-up ended when the supply of fertile, preconditioned lithospheric mantle was exhausted, at which time asthenosphere-derived, OIB-type volcanism became dominant. Miocene Arabia-Eurasia collision ended the extensional period and inverted the rift basins. Abbreviations: UD, Urumieh-Dokhtar magmatic belt; AB, Alborz Mountains; CI, central Iranian Eocene volcanics between Urumieh-Dokhtar and the Alborz Mountains.

7. CONCLUSION

Based on the studies, the rock units in the study include volcanic to plutonic masses with an alkaline nature. According to the lithographic studies, they have granular, intergranular, Poiclitic, and porphyroid texture. The geochemical investigations indicate the formation of the magma from the partial melting of 5 to 7% of a mantle source of uplifting peridotite garnet, at a depth of 100 to 105 km and the obvious role of separation crystallization as the main process in the formation of the magma forming these rocks. According to tectonic diagrams and tectonic studies, the rocks in the area have been formed in a post-collision inter-continental tensile environment. The volcanic rocks are the host of the Chaghoo copper orebody that originated in the final stages of rhyolite ore differentiation. The volcanic and plutonic rocks have been originated during the Eocene and Oligocene, respectively. The mineralization is resultant from the hydrothermal solutions related to the mentioned rocks in the last magmatic differentiation stage. However, the presence of faults and their role in the mineralization process has also been effective in this regard.

REFERENCES

- Adewumi, T., Adeyinka Salako, K., Defyan Alhassan, U., Abbass Adetona, A., Adewuyi Rafiu, A., Emeka Udensi, E. (2021). Interpretation of Airborne Radiometric data for possible hydrocarbon presence over Bornu basin and its environs, Northeast Nigeria using Thorium normalisation method, *Iranian Journal of Earth Sciences*, 13(3): 161-172. doi: 10.30495/ijes.2021.682863
- Aftabi, A., Atapour. H. (2000). Regional aspects of shoshonitic volcanism in Iran, *Episodes*, 23, 119–125.
- Agard, P., Omrani, J., Jolivet, L., Whitechurch, H., Vrielynck, B. (2011). Zagros orogeny: a subduction-dominated process, *Geological Magazine*, 148, 692-725.

Aldanmaz, E., Pearce, J. A., Thirlwall, M. F. & Mitchell, J. G. (2000). Petrogenetic evolution of late Cenozoic, post-collision volcanism in western Anatolia, Turkey. *Journal of Volcanology geothermal Research*, 102, 67-95.

Arampour, A., Afghah, M., Parvaneh Shirazi, M. (2021). Biostratigraphy and depositional architecture of the Kazhdumi formation (Aptian-Albian) in the Izeh zone, Zagros mountains, SW Iran, *Iranian Journal of Earth Sciences*, 13(3): 223-237. doi: 10.30495/ijes.2021.682869

Barahouei, B.A., Noura, M.R., Moslempour, M.E., Dabiri, R. (2021). Evaluation of groundwater suitability for the domestic and irrigation purposes in Konaro Ophiolitic Area, Iranshahr, SE Iran, , *Iranian Journal of Earth Sciences*, 13(3): 196-208. doi: 10.30495/ijes.2021.682867

Conder, J. A., Wiens, D. A., Morris, J. (2002). On the decompression melting structure at volcanic arcs and back - arc spreading centers, *Geophys. Res. Lett*, 29(15), 1727, doi:10.1029/2002GL015390.

Corbett, G.J. (2004). Epithermal and porphyry gold –geological models in Pacrim Congress 2004, Adelaide, Australia, *Institute of Mining and Metallurgy*, 15-23.

Cox, K.G., et al. (1979) The Interpretation of Igneous Rocks. Allen and Unwin, London, 450 p. <http://dx.doi.org/10.1007/978-94-017-3373-1>

Gaetani, G. A., & Grove, T. L. (2004). Experimental constraints on melt generation in the mantle wedge, in Inside the Subduction Factory, *Geophys. Monogr. Ser.*, 138, edited by J. Eiler, pp. 107–133, AGU, Washington, D. C.

Gardezi, S.A.H., Ahmad, S., Ikram, N., Rehman, G. (2021). Geological constraints on the Western Kohat foreland basin, Khyber Pakhtunkhwa, Pakistan: Implication from 2D and 3D structural modelling, *Iranian Journal of Earth Sciences*, 13(2): 61-76. doi: 10.30495/ijes.2021.678954

Guilbert, J.M., Park, C.F. (1986). The geology of ore deposits, *Freeman*. New York, p: 985.

Humphreys, E., Hessler, E., Dueker, K., Farmer, G. L., Erslev, E., & Atwater, T. (2003). How Laramide - age hydration of North American lithosphere by the Farallon slab controlled subsequent activity in the western United States, *Int. Geol. Rev.*, 45, 575–595, doi:10.2747/0020-6814.45.7.575.

Irvine, T., Baragar, W.R.A, (1971). A guide to the Chemical classification of the common volcanic rocks. *Canadian Journal of earth Science Letters*, 8, 523-548.

Jafari, J., Mahboubi, A., Moussavi-Harami, R. (2021). Seismic and sequence stratigraphy of the Oligocene-Miocene Asmari reservoir in the Marun oilfield, SW Iran, *Iranian Journal of Earth Sciences*, 13(2): 115-131. doi: 10.30495/ijes.2021.681581

Le Bas, M.J., Lemaitre, R.W., Streckeisen, A. & Zanettin, B. (1986). A Chemical Classification of Volcanic-Rocks Based on the Total Alkali Silica Diagram. *Journal of Petrology* 27(3): 745-750.

Le Roex, A. P., Dick H. J. B., Erlank A. J., Reid A. M., Frey F. A., & Hart S. R., (1983). Geochemistry, mineralogy and petrogenesis of lavas erupted along the south west Indian ridge between the Bouvet triple junction and 11 degrees east. *Journal of Petrol*, 24, 267-318.

- Morovati, F., Mirzaie Ataabadi, M., Arian, M., Zohdi, A., Al-e Ali, M. (2021). Age, microfacies and sedimentary environments of the Sirenia-bearing deposits of the Qom Formation in Central Iran, *Iranian Journal of Earth Sciences*, 13(2): 132-147. doi: 10.30495/ijes.2021.681579
- Olufemi, O. A., Mubor Yinka. A., Ismail Alao, E., Feyisayo Alexander, A. (2020). Magnetic rocks distribution and depth to basement analysis on an old Quarry Site, Abeokuta, SW Nigeria, *Iranian Journal of Earth Sciences*, 12(3), 176-183.
- Omrani, J., P. Agard, H. Whitechurch, M. Benoit, G. Prouteau, and L. Jolivet. (2008). Arc magmatism and subduction history beneath the Zagros Mountains, Iran: A new report of adakites and geodynamic consequences, *Lithos*, 106, 380–398, doi:10.1016/j.lithos.2008.09.008.
- Pearce, J. A. (1982). Trace element characteristics of lavas from destructive plate boundaries. John Wiley and Sons, U.K., pp. 525–548.177–195.28: 2023-2037.
- Pearce, J. A., & Parkinson. I. J., (1993). Trace element models for mantle melting: Application to volcanic arc petrogenesis, in *Magmatic Processes and Plate Tectonics*, edited by H. M. Prichard et al., *Geol. Soc. Spec. Publ*, 76, 373–403.
- Plank, T., & Langmuir, C. H. (1988). An evaluation of the global variations in the major element chemistry of arc basalts, *Earth Planet. Sci. Lett*, 90, 349–370, doi:10.1016/0012-821X(88)90135-5.
- Pourabdollahi, M., Dorostian, A., Rahimi, H., Eshaghi, A. (2021). Ground-motion simulation for the 2017 Mw7.3 Ezgeleh earthquake in Iran by using the Empirical Green's Function Method, *Iranian Journal of Earth Sciences*, 13(2): 148-158. doi: 10.30495/ijes.2021.681580
- Rajabi, M., Senemari, S., Parvaneh Nejad Shirazi, M., Bahrammanesh Tehrani, M. (2021). Depositional environment and microfacies analysis: An example of the Asmari Formation in West Zagros Basin, Lorestan province (Iran), *Iranian Journal of Earth Sciences*, 13(2): 94-114. doi: 10.30495/ijes.2021.681578
- Saeedi Razavi, B. (2021). Biostratigraphy, Paleoecology, Microfacies and Depositional environment of the Asmari formation (Oligocene-Early Miocene) in Karanj oil field, SW Iran, *Iranian Journal of Earth Sciences*, 13(3): 181-195. doi: 10.30495/ijes.2021.682865
- Shaw, D.M., (1970). Trace element fractionation during anatexis, *Geochim. Cosmochim. Acta*, 34, 237-243.
- Sisson, T. W., Bronto, T. (1998). Evidence for pressure - release melting beneath magmatic arcs from basalt at Galunggung, Indonesia, *Nature*, 391, 883–886, doi:10.1038/36087.
- Sun, S. S., & McDonough, W. F. (1989). Chemical and isotopic systematics of oceanic basalts: implications for mantle composition and processes” In: Saunders, A.D., Norry, M.J. (Eds.), *Magmatism in the Ocean Basins*. Geol Soc Spec Publ., Vol. 42, PP. 313-345.
- Talusani, V. R. (2010). Bimodal tholeiitic and mildly alkalic basalts from Bhir area, central Deccan Volcanic Province, India: Geochemistry and petrogenesis. *Journal of Volcanol. Geotherm. Res*, 189, 278-290.
- Ullah, H., Khalid, P., Mehmood, M., Ahmed Mashwani, S., Abbasi, Z., Jehangir Khan, M., Ul Haq, E., Mujtaba Shah, G.H. (2021). Reservoir potential, net pay zone and 3D modeling of Cretaceous Pab

Formation in Eastern Suleiman Range, Pakistan, *Iranian Journal of Earth Sciences*, 13(3): 173-180. doi: 10.30495/ijes.2021.682864

Verdel, C., Wernicke, B.P., Hassanzadeh, J. (2011). A Paleogene extensional arc flare-up in Iran, *Tectonics*, 30, 3.

Wang, Y.N., Zhang, C. J., Xiu. S.Z. (2001). Th/Hf-Ta/Hf identification of tectonic setting of basalts. *Acta Petrol Sin (in Chinese)*, 17(3), 413-421.

Widdowson, H.G. (1991). Aspects of Language Teaching. Oxford: OUP (1996). Teaching Language as Communication. Oxford: OUP. p 160.

Widdowson, M., Pringle M. S., & Fernandez O. A. (2000). A post K-T Boundary (Early Palaeocene) age for Deccan-type feeder dykes, Goa, *India J Petrol*, 41, 1177-1194.

Wood, D. A. (1980). The application of a Th-Hf-Ta diagram to problems of tectonomagmatic classification and to establishing the nature of crustal contamination of basaltic lavas of the British Tertiary volcanic province. *Earth Planet Sc Lett*, 50, 11-30.